

RoomStructNet: Learning to Rank Non-Cuboidal Room Layouts From Single View

Xi Zhang, Chun-Kai Wang, Kenan Deng, Tomas Yago-Vicente, Himanshu Arora
 Visual Search & AR
 Palo Alto, CA 94301

{xizhn,ckwang,kenanden,victomas,arorah}@amazon.com

Abstract

In this paper, we present a new approach to estimate the layout of a room from its single image. While recent approaches for this task use robust features learnt from data, they resort to optimization for detecting the final layout. In addition to using learnt robust features, our approach learns an additional ranking function to estimate the final layout instead of using optimization. To learn this ranking function, we propose a framework to train a CNN using max-margin structure cost. Also, while most approaches aim at detecting cuboidal layouts, our approach detects non-cuboidal layouts for which we explicitly estimate layout complexity parameters. We use these parameters to propose layout candidates in a novel way. Our approach shows state-of-the-art results on standard datasets with mostly cuboidal layouts and also performs well on a dataset containing rooms with non-cuboidal layouts.

1. Introduction

The problem of room layout estimation from a single image corresponds to identifying the extent of walls, floor, and ceiling of the depicted room as if it was empty. Room layout estimation is a fundamental component of indoor scene understanding that remains unsolved. Furthermore, it has recently gained great interest due to its direct application to holistic scene understanding [13, 14], robotic navigation [15] and augmented reality [4, 26].

The first stage of most existing approaches is to detect features to localize the layout, see Figure 1 left. For instance, classical approaches use vanishing point aligned line segments [9, 17], superpixels [31], or edges [21]. More recent works have replaced these bottom up image features with CNN based features learned from data, such as: informative edge maps [21, 25], location of boundaries where two room surfaces meet (e.g. wall-wall boundaries) [35, 36], location of corners where three room sur-

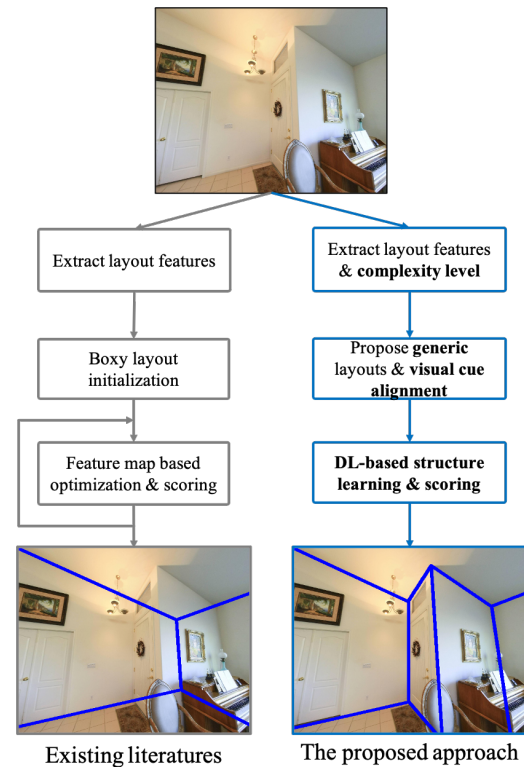


Figure 1. Comparison of layout prediction pipelines between existing literatures and the proposed approach. The proposed approach differs from existing literatures and has improvement at every step. We use bold font to highlight key contribution and difference of the proposed approach at each step.

faces meet (e.g. wall-wall-floor corner) [16, 36], segmentation masks of room surfaces [15, 2, 25] or depth maps of dominant planes [32, 27]. In a similar manner, we propose to use room boundaries, corners, and surface labels as features to learn. We believe these have complementary information that provides robustness to clutter, which will allow us to estimate better layouts.

After feature detection, most approaches use the detected

features to estimate a cuboidal layout, see Figure 1 left. Assuming the room to have a box shape allows for easier parameterization and solution search. Many approaches explicitly estimate orthogonal vanishing points and enforce walls to be oriented along these [9, 17, 21, 25]. Others assume existence of at most 3 walls while estimating surface labels [2, 25]. More recent approaches limit themselves only to layout configurations of visible walls, floor, and ceiling that can occur for a cuboidal layout [35]. Some approaches even detect the configuration explicitly from a predefined small set of cuboidal room layout types [16]. It is worth noting that not all rooms can actually be modeled as a box. This is especially true for modern homes with multi-functional rooms like living room/kitchen area or master bedroom/bathroom area. Hence, we propose a generic room layout model that can also handle such rooms with arbitrary number of walls. Additionally, as part of our feature extraction we propose to train a network to find the parameters of our generic layout model that best suit the given input image, see Figure 1 right. Moreover, we propose a novel sampling algorithm that generates plausible room layouts based on the estimated generic layout parameters and the attention provided by our robust learned features.

Recent approaches that attempted generalization to non-cuboidal layouts operate on panoramic images, whereas we operate on perspective images [36, 3]. The work in [12] uses a representation to detect non-cuboidal layouts which estimates the probability of wall-wall boundary locations and corners in a reprojected the image and uses it to sample layouts. Similarly, [27, 11] uses planes estimated by analyzing RGB or RGBD images to sample non-cuboidal layouts. In contrast to these works, our model explicitly outputs generic layout parameters such as number of visible walls and corners, instead of just sampling non-cuboidal layouts.

In order to estimate the room layout, most approaches either use heuristics or an optimization procedure guided by the layout features extracted in previous stages, see Figure 1 left. These can include aggregating detected features in layout regions [25], using physics inspired gradient descent on layout boundary confidence maps [35], greedy descent of layout boundaries using layout surface label confidence maps [2] or optimization using combined 2D and 3D cost functions [36, 27]. Layout structure is complex, it needs to satisfy many constraints such as perpendicularity of floor and walls, planar nature of each surface. Hence, it may require non-trivial combinations of multiple kinds of features. We do believe these combinations are best learned from data. For instance, to exploit the structured nature of a layout, the seminal work of [9] uses max-margin structured output regression to train a layout ranker as a linear combination of different kinds of features. Instead of a linear combination, we propose a neural network to score lay-

outs and rank them. In addition, we propose a novel way to train this neural network using max-margin structure cost. Comparing to methods [23] estimating generic layouts from 360° image, the proposed approach address generic layout estimation by using a single perspective image.

To evaluate our proposed method, we conduct experiments on the challenging Hedau [9] and LSUN [30] room layout benchmark datasets. Our method outperforms the current state of the art approach of Hsian *et al.* [12] in both datasets by a clear margin. Note that these datasets contain only cuboidal layouts ground truth annotations. Therefore, we created a new dataset with rooms with generic non-cuboidal layouts to fully evaluate the potential of our method. This dataset consists of a large collection images (50K) extracted from panoramas of the PanoContext [34] dataset and relabeled by us. Our method obtains impressive qualitative results on this more challenging unconstrained data, while achieving decent quantitative performance.

Our main contributions are:

1. We propose a novel generic room layout estimation system that achieves the state-of-the-art performance in both cuboidal and non-cuboidal/generic layout datasets.
2. We propose a non-cuboidal layout parametric representation able to handle increasingly complex layouts. For this, we explicitly learn to predict its complexity parameters.
3. We present a new way to generate layout candidates based on multiple kinds of feature maps, predicted layout complexity, and visual cue alignment.
4. We are, to the best of our knowledge, the first to propose using a deep neural network to rank candidate layouts. For this, we introduce a new framework to train a CNN using max-margin structure loss.

2. RoomStructNet for layout estimation

Our proposed system RoomStructNet takes an indoor scene image as an input, and estimates its non-cuboidal layout. We are able to handle complex non-cuboidal rooms thanks to our generic layout representation, detailed in Section 2.1.

We show a diagram of our full pipeline in Figure 2. In the first stage, RoomStructNet uses a network to detect robust layout features as confidence maps that encode layout boundaries, corners, and surface segmentations. This is shown by black arrows in Figure 2, and discussed in Section 2.2. In the next stage, RoomStructNet uses the computed robust features to generate candidate layouts, shown by gray arrows in Figure 2. We present our layout candidate generation methodology in Section 2.3. In the last stage, RoomStructNet embeds the candidate layouts jointly with their robust features, and scores them to select the final estimated layout. This process is shown by blue arrows in

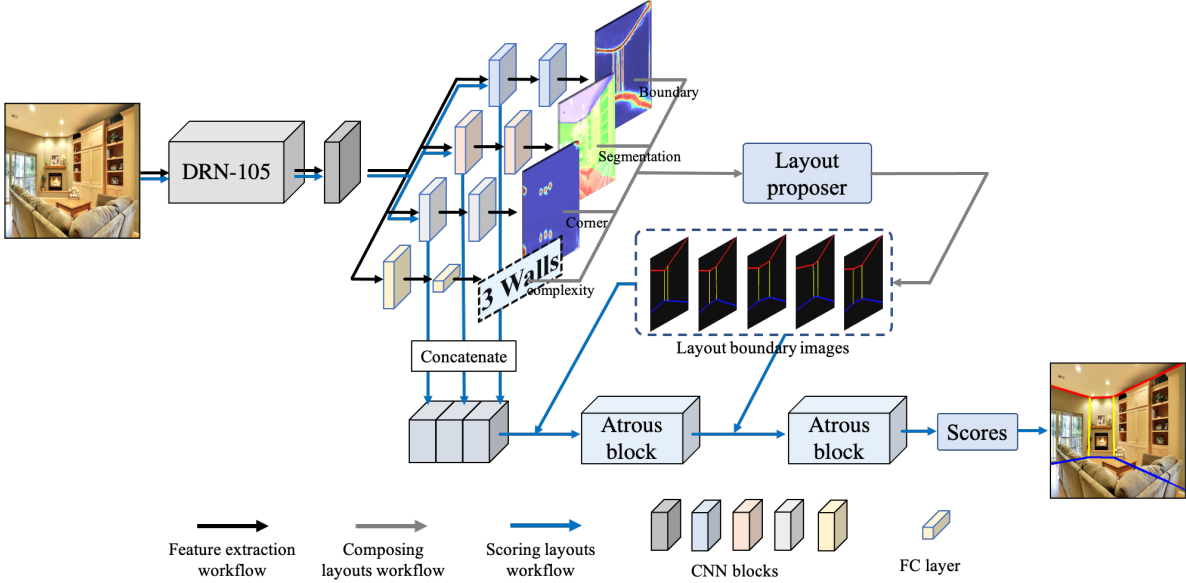


Figure 2. Our RoomStructNet pipeline. First, we predict different feature maps and the layout complexity level using a trained featured extraction network, whose process is shown by the black arrows. Second, we propose candidate layouts using the extracted features and the complexity level, shown by the grey arrows. Lastly, we score the candidate layout, shown by the blue arrow.

Figure 2, and described in Section 2.4.

2.1. Generic layout representation

Following the seminal work of Hedau et al. [9], most approaches attempt to estimate boxy layouts that segment an image into wall (w), ceiling (c) and floor (f) polygons. This is typically done by either sampling Manhattan rooms using orthogonal vanishing points, or relying upon 11 types of room layout configurations specified in the LSUN dataset [30]. Unlike previous works, here we propose a representation that makes no grossly simplifying assumptions about the captured room, such as perpendicularity of walls, the number of existing walls, or limited predefined room configurations. We only assume that all walls are vertical to the floor.

Given an image $I \in \mathbb{R}^{m \times n \times 3}$, we represent a layout L containing an arbitrary number of walls n as an ordered collection of wall-wall (ww) boundaries, which are defined by line segments $L = \{l_0^{ww}, l_1^{ww}, \dots, l_n^{ww}\}$. These line segments should all ideally intersect at the vertical vanishing point lying outside the image. Each segment l_i joins a wall-wall-floor (wwf) corner (x_i^f, y_i^f) with a wall-wall-ceiling (wwc) corner (x_i^c, y_i^c) . These corners can lie either inside the image if visible, or at image boundaries if not visible in the image. To account for ww boundaries for walls not fully visible in the image, we allow l_0 to lie on the left image boundary and l_n to lie on the right image boundary. Given the ww line segments, the i -th wf segment l_i^{wf} is computed by joining (x_i^f, y_i^f) and (x_{i+1}^f, y_{i+1}^f) . The floor polygon is computed by joining wwf corners and the image

boundaries. The wc boundaries and ceiling polygon can be constructed in a similar fashion. As a dual representation for layout L , we create a 3-channel layout boundary image I^L with each channel encoding one of ww , wf or wc boundaries.

2.2. Robust layout features extraction

Robust features are fundamental for correctly localizing candidate room layouts. As suggested by the success of recent works [35, 21, 36, 16], we advocate that these features are better learned from data.

Consequently, we propose using three kinds of such features together: boundary, corner and segmentation maps. We believe these complement each other in terms of information content and robustness. For instance, visible wall-wall and wall-ceiling boundaries are usually best captured by boundary confidence maps. While wall-wall-ceiling corners are best captured by corner confidence maps. Finally, occluded wall-floor boundaries and wall-wall-floor corners are best captured by analyzing the masks of occluding furniture items in segmentation maps.

Beyond estimating the aforementioned visual layout features, we propose using an additional network branch to predict the complexity of the scene depicted in the input image. We define room layout complexity as the number of visible walls in the scene. Since we perform semantic segmentation rather than instance segmentation, our segmentation maps do not separate different walls. Therefore, the predicted number of visible of walls nicely complements the segmentation information.

Our proposed RoomStructNet feature extraction module takes an image as an input, and predicts three per-pixel maps and one value representing layout complexity level (see Figure 2). The corner map, M_c , is a 2-channel image with pixel values expressing the confidence of detecting wwf and wwc corners, respectively, in each channel. The boundary map, M_b , is a 4-channel image where pixel values in each channel denote, respectively, the confidence of detecting ww , wf , and wc boundaries as well as non-boundary locations. The segmentation map, M_s , is a 3-channel image with each pixel labeled as wall w , floor f , or ceiling c . These labels are the result of a layout segmentation task, which ignores the occluding objects like furniture and labeling as if the room was empty. The module also outputs the predicted layout complexity level as a scalar \mathcal{C} , with $\mathcal{C} \geq 0$.

To extract these features we use a Dilated Residual Network (DRN) [29] with a configuration of 105 layers as our backbone network. To the network branches for corner, boundary, and segmentation prediction tasks, we add two convolutional layers with batchnorm and softmax in our network design. To the layout complexity level prediction branch, we add a fully connected layer at the end, which outputs the predicted number of visible walls.

We train our proposed feature extraction network in two stages. First, we train jointly the DRN-105 backbone and the subsequent network branches of all four tasks until convergence. Second, we fix parameters of the DRN-105 backbone, and follow by training each branch separately with a smaller learning rate. We employ L_2 regression loss for the layout complexity prediction task and binary cross entropy loss for the other three tasks. The total loss of the network is the sum of the losses of all four tasks.

2.3. Generic layout candidate generation

We pose the problem of layout estimation as an object detection task, where the goal is to detect the layout that best suits the input image. Deep learning based object detection methods can be broadly categorized into two groups. First, we have methods that pose object detection as a regression problem and adopt a unified framework to achieve the goal of either classifying or localizing objects [24, 19, 22]. And then, we have methods that follow the traditional object detection pipeline. That is, first target proposals are produced, and then each proposal is either classified or rank each into different object categories [6, 8, 5, 7]. Our proposed approach belongs to the second group: we first generate candidate layouts, and then we rank them to obtain the final layout estimate.

The goal of our layout candidate generation is to propose wide range of plausible generic layouts that can potentially fit the image with high accuracy. And we do this without the assumption of cuboidal room layout. To achieve this goal,

we adopt a two stage process. In the first stage, we initialize all possible layouts for the given predicted layout features and complexity level. In the second stage, we use different visual cues to fine-tune the initial layout candidates and increase the accuracy of their localization.

2.3.1 Candidate layout initialization

In contrast to many previous works [10, 9, 2], we do not assume that the layout is cuboidal, and hence we cannot initialize the layouts using a limited number of predefined layout templates. We instead rely upon the signals provided by layout features and complexity level predicted by our network described in Sec. 2.2 to initialize layouts.

During the training of our feature extraction network, we noticed that our prediction of boundary map M_b and layout complexity level \mathcal{C} is very precise for most cases – the prediction overestimates the number of walls in 16% of cases but never underestimates the number. So our initialization process uses predicted boundary as a starting point and produces room layout candidates with at most \mathcal{C} walls. We consider all possible combinations of presence of ceiling, walls and floors in an image during the initialization, which includes $\{c, w, f\}$, $\{c, w\}$, $\{w, f\}$ and $\{w\}$.

To begin with, our initialization process detects ww boundary candidates by using the boundary map M_b . Since ww boundaries are mostly visible and crisp in input images, line detection on M_b is straight forward. To detect these boundaries, we use image thresholding followed by morphological operation and line fitting on M_b .

To guarantee high recall for later stages, we also extract additional boundaries from the corner map M_c . For this, we first compute the vanishing points of the image corresponding to three principal orthogonal directions using approach introduced in [20]. Since we are not assuming the layout to be cuboidal, the vanishing points corresponding to horizontal room planes are not useful for us. We however assume the room walls to be vertical, hence we trust and use the vertical vanishing point in our work. Each pixel of our corner map M_c describes the confidence of detecting one of wwf , wwc corner types. We thus detect wwf corners and wwc corners by finding local maxima in M_c . We then create bipartite connections between every wwf and wwc corner pair. To select valid ww boundaries, we examine alignment between each ww boundary and the vertical vanishing point. When vanishing point is not successfully computed, the ww boundaries are compared with vertical direction. Figure 3 shows this process of extracting lines from M_c .

We then generate layout candidates using the detected ww boundaries. Suppose we detect N ww boundary candidates from the maps M_b and M_c using the approach described above. To propose a layout containing \mathcal{C} walls, we

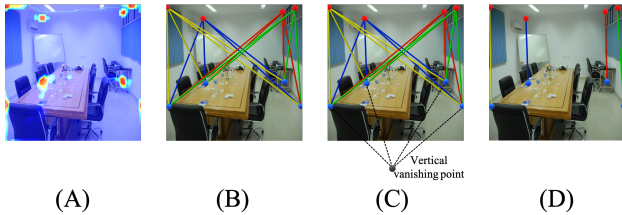


Figure 3. An illustration of the wall-wall boundaries proposing process. Given a predicted corner map, as shown in (A), we extract all local maximum as corner candidates and construct bipartite connections between the ceiling corners and the floor corners, as shown in (B). We then compare each ceiling-floor connection with the vertical vanishing point, shown in (C), and select the final wall-wall boundaries that follow the vanish point constraint, shown in (D).

first select $C - 1$ of the N ww boundary candidates. We then find the top and bottom point for each ww boundary line segment, corresponding to the wwc and wwf corner, using the floor and ceiling regions of the surface segmentation mask M_s . We illustrate this process in Figure 4. First we find the intersection between each ww line and region boundaries in M_s . If any intersection is too close to an image edge, we will instead replace it with the junction between ww and the image boundary. Finally, we connect the ceiling and floor points in order to form ceiling and floor regions respectively. At the end of the initialization process we obtain many layout candidates.

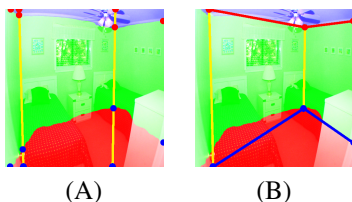


Figure 4. An example of layout initialization using ww boundaries and M_s segmentation mask. (A) First, we compute the intersections between ww and M_s mask. If any intersection is too close to an image boundary, we will set it to the intersection of ww and the same boundary. (B) We initialize a layout by connecting ceiling and floor intersections.

2.3.2 Visual cue alignment for layout candidate refinement

So far we have obtained a collection of initialized layouts $\mathbf{L} = \{L_i\}_{i=0}^n$ of the given input image. Many previous works conduct an optimization process that iteratively move layout connection joints to achieve better score and select the layout with best score as the final output.

Although an optimization process can improve layout accuracy, it also comes with drawbacks. First, it is computationally expensive and sometime requires a heuristic

stopping criteria. Secondly, many works use the predicted feature map as the optimization space, which often leads to local minimas due to lack of actual visual signals.

Instead of executing an iterative optimization process, we refine the candidates by aligning layout lines to visible cues in the scene, as illustrated in Figure 5. We first extract all visible line segments from the input image, and then align the initial layout boundaries to nearby line segments. We log all intermediate layouts and treat them as layout candidates as well.

Our refinement procedure should in theory produce similar or better results compared to an optimization-based approach. For scenes without occlusion, the layout initialization described in the previous section can already generate accurate layouts without additional refinement. For scenes with completely occluded layout boundaries and corners, an optimization process lacks additional signal compared to the feature extraction network. For scenes with partial occlusions, since some parts of layout lines and corners are still visible and detectable, our alignment-based approach has direct signals to improve the layout candidates. Our experiment results also validate our hypothesis here.

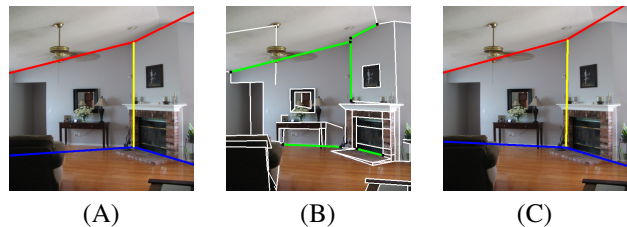


Figure 5. An example of the visual cues alignment process. Given an initial layout propose in (A), we generate an layout aligned to the visual cues in (C). We show all computed visual cues in (B) and highlight the line segments used for alignment in green.

2.4. Candidate layout scoring using CNNs

Given an image I and a layout L_i proposed by the methodology described in Sec. 2.3, we want to determine whether it is a correct layout for the image. One approach is to pose this task as classifying the layout as correct or not, but proposing the ground truth layout is difficult. Instead, like most prior works, we formulate this task as learning a scoring function $f_s(L_i, I)$ that will assign a higher score to a layout more similar to the ground truth.

We illustrate the layout scoring process with the blue arrows in the network architecture in Figure 2. To jointly embed the image and a layout, we take concatenated network outputs from one layer before the layout features (described in Section. 2.2) and append them with the layout boundary image I^{L_i} produced from the candidate layout. We then pass it through a network with two Atrous residual blocks [1] to generate the final layout score. To reinforce the information provided by the candidate layout, we

again append I^{L_i} to the network output between the two Atrous residual blocks. Given a set of proposed layouts $\mathbf{L} = \{L_i\}_{i=1}^n$, our system selects the layout with the maximum score as the output:

$$L^* = \arg \max_{L_i \in \mathbf{L}} f_s(L_i, \mathbf{I}).$$

Training using max-margin structure cost. Room layout is more than just a classification label; it is a complex construct containing structural information of the scene, such as location and orientation of layout lines and their intersections. In this structured space, layouts which are closer to the ground truth should be penalized less than those further away. Thus we use the max-margin structure cost inspired by [33, 18] to train our network, which forces the score of the ground truth layout \hat{L} of an image \mathbf{I} to be larger than that of another layout L_i by a margin $\Delta(L_i, \hat{L})$, a non-negative function computing the deviation between two layouts. In this setup, we aim to minimize the structure cost

$$E(L_i) = \max \left(0, f_s(L_i, \mathbf{I}) + \Delta(L_i, \hat{L}) - f_s(\hat{L}, \mathbf{I}) \right).$$

For the cost function, we minimize the cost for all available layouts, as described in Eq. 2. In the original Support Vector formulation in [28], the authors minimize the cost while maintaining margin constraints by using only the layout that violates the margin constraint the most, as described in Eq. 1. In their setup, this drastically reduces the number of constraints and hence the linear system of equations to be solved in each iteration. However, for our neural network formulation this adds complexity of search to otherwise differential formulation. We thus chose to adopt Eq. 2, which leads to faster convergence and allows more training samples and constraints to be utilized.

$$C_1 = \max_i E(L_i) \quad (1)$$

$$C_2 = \sum_i E(L_i) \quad (2)$$

Computing the margin $\Delta(\cdot)$. Our margin function computes the deviation of a layout L_i from the ground truth layout \hat{L} as a combination of a line-based deviation and area-based deviation, as described in Eq. 3. The line based deviation computes the distance between the respective layout boundaries of the two layouts, by summing the pixel distance and angular distance, as described in Eq. 4. To compute the area based deviation, we first convert a layout to the floor/wall/ceiling area masks, denote as $\{M^f, M^w, M^c\}$ respectively, by constructing the wall, ceiling and floor polygons as described in Sec. 2.1. We then compute D_{area} as defined in Eq. 5, where the first term computes the area shrunk in prediction compared with the ground truth, and

the second term computes Intersection-over-Union (IOU). In practice, we only consider the floor mask in the computation because floor affordance is more important in most applications.

$$\Delta(L_i, \hat{L}) = D_{line}(L_i, \hat{L}) + D_{area}(L_i, \hat{L}) \quad (3)$$

$$D_{line}(L_i, \hat{L}) = \|L_i, \hat{L}\|^2 + \cos(L_i, \hat{L}) \quad (4)$$

$$D_{area}(L_i, \hat{L}) = \sum_{\alpha \in \{f, w, c\}} 2 - \frac{|M_i^\alpha \cap \hat{M}^\alpha|}{|\hat{M}^\alpha|} - \frac{|M_i^\alpha \cap \hat{M}^\alpha|}{|M_i^\alpha \cup \hat{M}^\alpha|} \quad (5)$$

3. Experiments

In this section, we show our experiment setup and discuss results of the proposed approach.

3.1. Datasets

We evaluated the proposed approach on two challenging room layout benchmarks: Hedau dataset [9] and LSUN scene understanding dataset [30]. Hedau dataset consists of 209 training images and 105 testing images. LSUN is a relatively larger dataset, consisting of 4000 training images, 394 validation images, and 1000 testing images. Both benchmarks assume cuboidal layouts in images. Since Hedau dataset contains too few training images, we did not train the network separately on this dataset. We instead followed the previous works [31, 15, 35] and performed testing on both LSUN and Hedau datasets using the model trained only on LSUN dataset.

To show that the proposed approach can predict generic non-cuboidal layouts, we also evaluated the approach on a new room layout dataset that we created using PanoContext dataset [34]. The original PanoContext dataset consists of 700 full-view panoramas with 418 bedrooms and 282 living rooms. The original annotations make the Manhattan world assumption [37] and contain only cuboidal layouts. To generate the new dataset, we selected 526 panoramas from the original dataset and relabeled the dataset without the Manhattan and cuboidal layout assumption. Then given a relabeled panorama, which covers 360 degrees in longitude and 180 degrees in latitude, we randomly sampled 6 perspective views every 24 degrees in longitude with FOV uniformly distributed between 70 and 120 degrees. Using this process, we generated 47,340 perspective views with layout labels, and we splitted panorama views to training and testing sets and generated 40,000 training and 7,340 testing perspective views. Examples of relabeled panorama and sampled perspective views are shown in Figure 6.

3.2. Evaluation results

Similar to most other works, we evaluated the performance of our approach using the following two metrics:

- e_{pixel} : Ratio of pixelwise error between predicted w, c, f areas and ground truth areas, normalized by the image size.



Figure 6. An example of a relabeled panorama and perspective views sampled from it. Upper left: the original labeling for the panorama. Bottom left: our retouched labeling. Right: perspective views sampled from the panorama.

Method	e_{pixel}	e_{corner}
Hedau <i>et al.</i> . (2009) [9]	24.23	15.48
Mallya <i>et al.</i> . (2015) [21]	16.71	11.02
Dasgupta <i>et al.</i> . (2016) [2]	10.63	8.20
Ren <i>et al.</i> . (2016) [25]	9.31	7.95
Hsian <i>et al.</i> . (2019) [12]	6.68	4.92
Hirzer <i>et al.</i> . (2020) [10]	7.79	5.84
Ours w/o visual cue alignment	7.32	5.03
RoomStructNet	6.21	4.65

Table 1. Quantitative results on LSUN. The proposed approach achieved the best results compared to both existing approaches and the proposed approach without using visual cue alignment.

- e_{corner} : Ratio of euclidean distance between positions of predicted layout joints and positions of ground truth joints, normalized by the image diagonal.

We present the results of the proposed approach and other approaches on LSUN dataset in Table 1 and Hedau dataset in Table 2. For LSUN dataset, the ground truth testing set is no longer available on the official evaluation kit. We thus evaluated only on the validation set (also the case with [16, 25, 36]). To verify and highlight the performance gain achieved by visual cue alignment, we conducted an ablation study by skipping the visual cue alignment in the proposed workflow (results also included in Table 1 and Table 2). Note that we excluded [35] in our comparison, as it used training data not provided in the benchmark and is thus not directly comparable to the other works.

We also show the qualitative results of the proposed approach on LSUN dataset in Figure 7. It performs well in highly cluttered scenes.

3.3. Results on generic room images

One advantage of the proposed approach is that it can predict non-cuboidal room layouts. Many works addressed generic room layouts prediction in the past. But they either assumed camera model exists in the data and used camera

Method	e_{corner}
Hedau <i>et al.</i> . (2009) [9]	21.2
Mallya <i>et al.</i> . (2015) [21]	12.83
Dasgupta <i>et al.</i> . (2016) [2]	9.73
Ren <i>et al.</i> . (2016) [25]	8.67
Hsian <i>et al.</i> . (2019) [12]	5.01
Hirzer <i>et al.</i> . (2020) [10]	7.44
Ours w/o visual cue alignment	6.55
RoomStructNet	4.81

Table 2. Quantitative results on Hedau dataset.



Figure 7. Qualitative results of the proposed approach on LSUN dataset.

pose in their approaches [11, 27] or conducted their prediction work on panoramic views [3, 37, 23]. The only work we found has a similar problem setup as us is [12], however we could not find the code of their approach online. At this point, to demonstrate this, we evaluated the performance of the proposed approach on the perspective views derived from PanoContext dataset and present results here by using the same evaluation metrics. We present some of qualitative results from our experiment in Figure 8. We also present qualitative results of layout feature maps extracted from room with generic layouts in Figure 9. It can be observed from the feature maps that the proposed feature extractor is capable of crisply detecting and locating layout features of given rooms, which enables the capability of detecting the generic layouts in the proposed approach.

We believe that the proposed complexity factor which controls the number of walls in predicted layouts plays an important role in generating final layouts. To better understand the impact of the complexity factor to the predicted layouts. We conducted an evaluation in which we included versions of our proposed approach with \mathcal{C} set to different numbers. Worth noting that by setting the complexity factor \mathcal{C} to 3, the proposed approach will only predict cuboidal layouts. Table 3 summarizes the results described above. We notice that the improvement becomes ignorable when



Figure 8. Qualitative results of the proposed approach on perspective views extracted from the relabeled PanoContext dataset. It can be observed from the figure that the proposed approach can handle non-cuboidal layouts of the datasets.

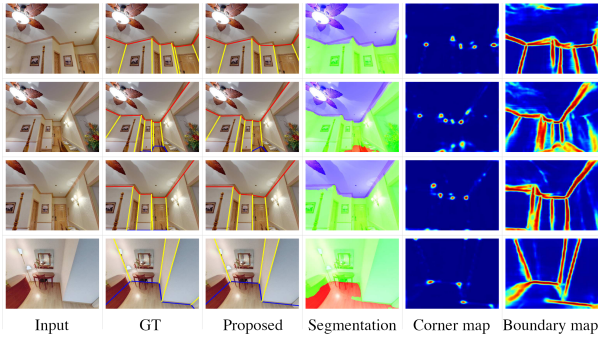


Figure 9. Examples of showing that the proposed layout feature extractor can detect layout features from rooms with generic layouts.

$\mathcal{C} > 6$. This is because for most of room images in our relabeled panoContext dataset has the number of walls less than or equal to 6. The proposed approach achieves better performance thanks to its ability to predict generic layouts. Some qualitative results of using different upper bounds for the complexity factor is shown in Figure 10.

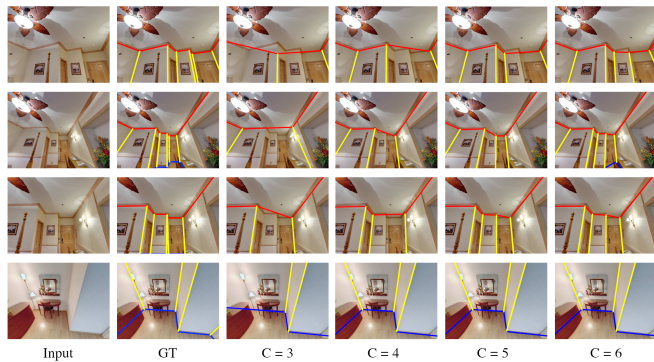


Figure 10. Qualitative results of setting different upper bounds for complexity factor \mathcal{C} .

3.4. Structure loss V.S. regression loss

While the proposed approach achieves superior performance by training layout scoring network using max margin structure loss, an alternative way is to train the network as a regression function that fits the layout margin we de-

Method	e_{pixel}	e_{corner}
RoomStructNet, $\mathcal{C} = 3$	11.32	8.12
RoomStructNet, $\mathcal{C} = 4$	10.97	7.81
RoomStructNet, $\mathcal{C} = 5$	9.74	6.92
RoomStructNet, $\mathcal{C} = 6$	9.37	6.54

Table 3. Quatitative results on perspective views derived from PanoContext dataset.

fin in Eq. 4. To compare, we trained the same network using the same LSUN layout candidate set extracted from the layout proposal process, with the loss function changed from structure loss to standard L2 loss. We then computed the average e_{pixel} (%) for Top 1, 5, 10, 20 layouts ranked by the trained networks. We examined multiple top layouts because a good layout scorer should still select a high quality candidate even when it does not select the best one. We hypothesize that the network trained with the structure loss can better achieve this desired property as it learns the order relationship among input layouts. The experiment results, summarized in Table 4, validates our hypothesis. It shows that the error rate for the network trained with the strcuture loss increases more slowly than the one with L2 loss.

Loss type	Top 1	Top 5	Top 10	Top 20
L2 loss	4.82	5.26	6.94	9.52
Structure loss	4.65	4.82	6.71	9.52

Table 4. A comparison between layout scoring networks trained using two different loss functions. We report the average e_{pixel} (%) for the top-k layouts ranked by the trained network on LSUN dataset.

4. Conclusion

In this paper, we present a new approach to estimate the layout of a room from its single image. While most of the recent approaches for this task use robust features learnt from data, they resort to optimization when detecting the final layout. In addition to using learnt robust features, the proposed approach learns an additional ranking function to estimate the final layout instead of using optimization. To learn this ranking function, we propose a framework to train a deep neural network using max-margin structure cost. Also, while most approaches aim at detecting cuboidal layouts, our approach detects non-cuboidal layouts for which we explicitly estimates layout complexity parameters. We use these parameters to propose layout candidates in a novel way. Our approach shows state-of-the-art results on standard datasets with mostly cuboidal layouts and also performs well on a dataset containing rooms with non-cuboidal layouts.

References

- [1] Liang-Chieh Chen, Yukun Zhu, George Papandreou, Florian Schroff, and Hartwig Adam. Encoder-decoder with atrous separable convolution for semantic image segmentation. In *Proceedings of the European conference on computer vision (ECCV)*, pages 801–818, 2018.
- [2] Saumitro Dasgupta, Kuan Fang, Kevin Chen, and Silvio Savarese. Delay: Robust spatial layout estimation for cluttered indoor scenes. In *Proceedings of the IEEE conference on computer vision and pattern recognition*, pages 616–624, 2016.
- [3] Clara Fernandez-Labrador, Jose M Facil, Alejandro Perez-Yus, Cédric Démonceaux, Javier Civera, and Jose J Guerrero. Corners for layout: End-to-end layout recovery from 360 images. *IEEE Robotics and Automation Letters*, 5(2):1255–1262, 2020.
- [4] Ran Gal, Lior Shapira, Eyal Ofek, and Pushmeet Kohli. Flare: Fast layout for augmented reality applications. In *2014 IEEE International Symposium on Mixed and Augmented Reality (ISMAR)*, pages 207–212. IEEE, 2014.
- [5] Ross Girshick. Fast r-cnn. In *Proceedings of the IEEE international conference on computer vision*, pages 1440–1448, 2015.
- [6] Ross Girshick, Jeff Donahue, Trevor Darrell, and Jitendra Malik. Rich feature hierarchies for accurate object detection and semantic segmentation. In *Proceedings of the IEEE conference on computer vision and pattern recognition*, pages 580–587, 2014.
- [7] Kaiming He, Georgia Gkioxari, Piotr Dollár, and Ross Girshick. Mask r-cnn. In *Proceedings of the IEEE international conference on computer vision*, pages 2961–2969, 2017.
- [8] Kaiming He, Xiangyu Zhang, Shaoqing Ren, and Jian Sun. Spatial pyramid pooling in deep convolutional networks for visual recognition. *IEEE transactions on pattern analysis and machine intelligence*, 37(9):1904–1916, 2015.
- [9] Varsha Hedau, Derek Hoiem, and David Forsyth. Recovering the spatial layout of cluttered rooms. In *2009 IEEE 12th international conference on computer vision*, pages 1849–1856. IEEE, 2009.
- [10] Martin Hirzer, Vincent Lepetit, and PETER ROTH. Smart hypothesis generation for efficient and robust room layout estimation. In *Proceedings of the IEEE/CVF Winter Conference on Applications of Computer Vision*, pages 2912–2920, 2020.
- [11] Henry Howard-Jenkins, Shuda Li, and Victor Prisacariu. Thinking outside the box: generation of unconstrained 3d room layouts. In *Asian Conference on Computer Vision*, pages 432–448. Springer, 2018.
- [12] Chi-Wei Hsiao, Cheng Sun, Min Sun, and Hwann-Tzong Chen. Flat2layout: Flat representation for estimating layout of general room types. *arXiv preprint arXiv:1905.12571*, 2019.
- [13] Siyuan Huang, Siyuan Qi, Yinxue Xiao, Yixin Zhu, Ying Nian Wu, and Song-Chun Zhu. Cooperative holistic scene understanding: Unifying 3d object, layout, and camera pose estimation. *arXiv preprint arXiv:1810.13049*, 2018.
- [14] Siyuan Huang, Siyuan Qi, Yixin Zhu, Yinxue Xiao, Yuanlu Xu, and Song-Chun Zhu. Holistic 3d scene parsing and reconstruction from a single rgb image. In *Proceedings of the European Conference on Computer Vision (ECCV)*, pages 187–203, 2018.
- [15] Hamid Izadinia, Qi Shan, and Steven M Seitz. Im2cad. In *Proceedings of the IEEE Conference on Computer Vision and Pattern Recognition*, pages 5134–5143, 2017.
- [16] Chen-Yu Lee, Vijay Badrinarayanan, Tomasz Malisiewicz, and Andrew Rabinovich. Roomnet: End-to-end room layout estimation. In *Proceedings of the IEEE International Conference on Computer Vision*, pages 4865–4874, 2017.
- [17] David C Lee, Abhinav Gupta, Martial Hebert, and Takeo Kanade. Estimating spatial layout of rooms using volumetric reasoning about objects and surfaces. In *Proceedings of the 23rd International Conference on Neural Information Processing Systems-Volume 1*, pages 1288–1296, 2010.
- [18] Sijin Li, Weichen Zhang, and Antoni B Chan. Maximum-margin structured learning with deep networks for 3d human pose estimation. In *Proceedings of the IEEE international conference on computer vision*, pages 2848–2856, 2015.
- [19] Wei Liu, Dragomir Anguelov, Dumitru Erhan, Christian Szegedy, Scott Reed, Cheng-Yang Fu, and Alexander C Berg. Ssd: Single shot multibox detector. In *European conference on computer vision*, pages 21–37. Springer, 2016.
- [20] Xiaohu Lu, Jian Yaoy, Haoang Li, Yahui Liu, and Xiaofeng Zhang. 2-line exhaustive searching for real-time vanishing point estimation in manhattan world. In *2017 IEEE Winter Conference on Applications of Computer Vision (WACV)*, pages 345–353. IEEE, 2017.
- [21] Arun Mallya and Svetlana Lazebnik. Learning informative edge maps for indoor scene layout prediction. In *Proceedings of the IEEE international conference on computer vision*, pages 936–944, 2015.
- [22] Mahyar Najibi, Mohammad Rastegari, and Larry S Davis. G-cnn: an iterative grid based object detector. In *Proceedings of the IEEE conference on computer vision and pattern recognition*, pages 2369–2377, 2016.
- [23] Giovanni Pintore, Marco Agus, and Enrico Gobbetti. Atlantanet: Inferring the 3d indoor layout from a single 360 degree image beyond the manhattan world assumption. In *European Conference on Computer Vision*, pages 432–448. Springer, 2020.
- [24] Joseph Redmon, Santosh Divvala, Ross Girshick, and Ali Farhadi. You only look once: Unified, real-time object detection. In *Proceedings of the IEEE conference on computer vision and pattern recognition*, pages 779–788, 2016.
- [25] Yuzhuo Ren, Shangwen Li, Chen Chen, and C-C Jay Kuo. A coarse-to-fine indoor layout estimation (cfile) method. In *Asian Conference on Computer Vision*, pages 36–51. Springer, 2016.
- [26] Misha Sra, Sergio Garrido-Jurado, Chris Schmandt, and Pattie Maes. Procedurally generated virtual reality from 3d reconstructed physical space. In *Proceedings of the 22nd ACM Conference on Virtual Reality Software and Technology*, pages 191–200, 2016.
- [27] Sinisa Stekovic, Shreyas Hampali, Mahdi Rad, Sayan Deb Sarkar, Friedrich Fraundorfer, and Vincent Lepetit. General

- 3d room layout from a single view by render-and-compare. In Andrea Vedaldi, Horst Bischof, Thomas Brox, and Jan-Michael Frahm, editors, *Computer Vision – ECCV 2020*, pages 187–203, Cham, 2020. Springer International Publishing.
- [28] Ioannis Tsochantaridis, Thomas Hofmann, Thorsten Joachims, and Yasemin Altun. Support vector machine learning for interdependent and structured output spaces. In *Proceedings of the twenty-first international conference on Machine learning*, page 104, 2004.
- [29] Fisher Yu, Vladlen Koltun, and Thomas Funkhouser. Dilated residual networks. In *Proceedings of the IEEE conference on computer vision and pattern recognition*, pages 472–480, 2017.
- [30] Fisher Yu, Ari Seff, Yinda Zhang, Shuran Song, Thomas Funkhouser, and Jianxiong Xiao. Lsun: Construction of a large-scale image dataset using deep learning with humans in the loop. *arXiv preprint arXiv:1506.03365*, 2015.
- [31] Jian Zhang, Chen Kan, Alexander G Schwing, and Raquel Urtasun. Estimating the 3d layout of indoor scenes and its clutter from depth sensors. In *Proceedings of the IEEE International Conference on Computer Vision*, pages 1273–1280, 2013.
- [32] Weidong Zhang, Wei Zhang, and Yinda Zhang. Geolayout: Geometry driven room layout estimation based on depth maps of planes. In *European Conference on Computer Vision*, pages 632–648. Springer, 2020.
- [33] Yuting Zhang, Kihyuk Sohn, Ruben Villegas, Gang Pan, and Honglak Lee. Improving object detection with deep convolutional networks via bayesian optimization and structured prediction. In *Proceedings of the IEEE Conference on Computer Vision and Pattern Recognition*, pages 249–258, 2015.
- [34] Yinda Zhang, Shuran Song, Ping Tan, and Jianxiong Xiao. Panocontext: A whole-room 3d context model for panoramic scene understanding. In *European conference on computer vision*, pages 668–686. Springer, 2014.
- [35] Hao Zhao, Ming Lu, Anbang Yao, Yiwen Guo, Yurong Chen, and Li Zhang. Physics inspired optimization on semantic transfer features: An alternative method for room layout estimation. In *Proceedings of the IEEE conference on computer vision and pattern recognition*, pages 10–18, 2017.
- [36] Chuhan Zou, Alex Colburn, Qi Shan, and Derek Hoiem. Layoutnet: Reconstructing the 3d room layout from a single rgb image. In *Proceedings of the IEEE Conference on Computer Vision and Pattern Recognition*, pages 2051–2059, 2018.
- [37] Chuhan Zou, Jheng-Wei Su, Chi-Han Peng, Alex Colburn, Qi Shan, Peter Wonka, Hung-Kuo Chu, and Derek Hoiem. Manhattan room layout reconstruction from a single 360 degree image: A comparative study of state-of-the-art methods. *International Journal of Computer Vision*, 129(5):1410–1431, 2021.